The Degree of Master of Science in Pharmacy

Thesis

Real-time monitoring of host-gut microbial interaction in anticancer drug metabolism

August 2021

Mai Van Hieu

Natural Products Science Major, College of Pharmacy

Master of Science Course in the Graduate School,

Seoul National University

Real-time monitoring of host-gut microbial interaction in anticancer drug metabolism

Under the Guidance of Prof. Park Sunghyouk
Submitted to the Faculty of Graduate School
Seoul National University, Korea

By
Mai Van Hieu
Pharmacy in Natural Products Science Major
Master of Science Course in the Graduate School
Seoul National University, Korea

Approved as a Qualified Thesis of Mai Van Hieu
For the degree of Master of Science in Pharmacy
By the Committee Members
August 2021

CHAIRMAN

VICE-CHAIRMAN

MEMBER

Abstract

Real-time monitoring of host-gut microbial interaction in anticancer drug metabolism

MAI VAN HIEU

Natural Products Science Major

College of Pharmacy

The Graduate School

Seoul National University

In humans, the microbiome can extensively impact the prevention, diagnosis, and treatment of various diseases. Recent studies have shown the critical implication of the gut microbiome to the efficacy and toxicity of different orally-administrable drugs in cancer treatment by back-and-forth interaction with the host. Despite enormous recent advances in the metabolism-related human gut microbiome, it remains various limitation to comprehensively monitor and evaluate the host-gut microbial interaction in response to chemotherapeutic materials depending on time. Therefore, we developed *in vivo* ^{19}F-NMR technique as an applicable method for real-time monitoring and qualifying the catabolism process of 5-FU in living biological inter-species system as *Caenorhabditis elegans* (*C. elegans*) and gut microbiome *Escherichia coli OP50 (OP50)*. The method exhibited the observable catabolism pathway of 5-FU on *C. elegans* fed *OP50*, in particular in the real-time kinematic consumption of 5-FU generating to different inactivated metabolites, including α-fluoro-β-ureidopropionic acid (FUPA) and (α-fluoro-β-alanine) FBAL by obtaining ^{19}F-NMR spectrum. *OP50* could catabolize 5-FU to 5,6-dihydro-5-fluorouracil (FUH2), a first intermediate in the catabolic cascade of 5-FU, proven containing DPD ortholog enzyme. *Escherichia coli JW2113 preT/preA deletion*

(*preT/preA* KO) was recruited to confirm the biological activity of *E. coli* DPD ortholog enzyme in 5-FU catabolism on the metabolite level by ^{19}F-NMR, and utilized as a microbial control model for separating the catabolism of 5-FU on *C. elegans-only* from the host-gut microbial system.

Regarding recruiting and analyzing relative NMR peaks, *C. elegans'* microbiome can incorporate into the pathway of 5-FU catabolism on the host by co-metabolizing and contributing FUH_2. In addition, the method was successfully applied and showed relevance on the human gut microbiome, including *E. coli KCTC 1116, MG1655,* and commercial probiotics. By developing *in vivo* real-time ^{19}F-NMR-based biological systems, this study thoroughly detailed the interaction between the gut microbiome containing 5-FU catabolic enzymes and the host in the catabolism of 5-FU. This applicable method should be generalized as a potential approach to monitoring the interaction between the host and gut microbes containing human-homologous enzymes in the systemic metabolism of fluorine-containing cancer drugs.

keywords : Real-time NMR, ^{19}F-NMR, inter-species interaction, *Caenorhabditis elegans*, gut microbiome, 5-FU, metabolism

***Student Number* : 2019-20500**

Table of Contents

Introduction

Inter-species interaction is the fundamental foundation of the dynamic life of all living creatures, well-known as symbiotic and competitive relationships, respectively. In the living system, the human cannot be separated from the interaction with other organisms consisting of not only multicellular organisms but also microorganisms. In 2001, Joshua Lederberg defined the concept of microorganisms closely interplaying with humans, called "human microbiome" in particular, which indicates the collection of entire microorganism genomes lively-habituating in the internal body cavity or surrounding surface of the human (1, 2). In recent days, the gut microbiome – the largest assemblage of microbes on humans - becomes an increasing trend of scientific research in the world (3). Notably, the host-gut microbial interaction has emerged as a potential aspect in the concept of microbiome being deeply concerned in the future (4).

Consisting of more than 10.000 species, and over 100 trillion microbial cells occupied by each adult, the human microbiome has been launched to various human growing processes (5, 6). Since birth, the infant gut microbial inhabitants have been established from the represented maternal microbiota, then evolve throughout the development of human life (7). In a healthy state, the most typical interplay between gut microbiota and the host is the symbiosis, or mutually beneficial relationship. As a role of host, the human can shape and modulate the development, composition, and function of the gut microbial community by their genetic feature (8, 9), nutrient intervention (10, 11), lifestyle (12). The gastrointestinal (GI) tract basically provides specific living environments and suitable growth conditions for the multitude of microorganism species. Regarding the biological characteristics among different sites along the length of the GI tract, the abundance of microbial community unevenly varies from mouth to colon (6, 13). In the GI tract, the food regularly passing through also becomes the primary source of nutrients for gut flora. In addition, gut microorganisms are also exposed to human intestinal excretion, some

of the essential nutrients for growth. In other words, colonized microorganisms make the intestinal tract their home. Given the close mutual relationship with the host, the gut microbiome also offers various beneficial interactions to human health and disease development. In fact, the vast microbial population and gene-rich ecosystem become the fundamental properties of interaction from gut microbiome. In this instance, the human immune system is established and fortified along with the repertoire of the microbiota as a diverse source of antigens (14). The accumulation of microbial colonization on the surface of the GI tract forms the first physical barrier encompassing the outer mucus layer, contributes to functional drive, and maintains the integrity of the intestinal membrane (15, 16). Moreover, gut microbes multiply rapidly and continuously, and they also provide an intrinsic source of necessary nutrients for the host such as certain vitamins, amino acids, minerals, carbohydrates (17-20). In fact, the gut microbiota showed the potential of involvement, contribution, and influence to various systemic metabolism pathways on humans, some are unique and indispensable.

During the last decades of discovery, drug metabolism remains an area of great concern and becomes an inseparable aspect in the overall perspective of the gut microbiome. Indeed, the GI tract, especially both the small and large intestine, is an essential station in the metabolism pathway of almost oral-administrative or liver-metabolized drugs. Throughout the gastrointestinal tract, a large accumulation of microbiota has a favorable opportunity to expose, and then interact with intestinal-circulation substances (21). By both direct and indirect diverse mechanisms, the gut microbiome may alter the pathway of drug metabolism, then influence the efficacy and toxicity of drugs by competing or contributing drug-metabolizing enzymes, activating with halting metabolites, regulating host-expressing proteins, or directly completing biotransformation of drugs (21-24). Through various analysis pipelines, the emerging shreds of evidence implicate the gut microbiome as the second genome of humans with an abundance of homologous genes encoding human metabolizing

enzymes (25, 26). So that, the complex of gut microbial community showed profound potential in metabolizing oral-administrative drugs. Therefore, most of the previous studies have focused on the contribution of microbiota to drug metabolism. However, in addition to acknowledgment, several studies have persuaded of the bidirectional relation of gut microbiome-host tissues in drug metabolism. The completed pathway of drug metabolism undergoes host-microbial interaction through multifaceted mechanisms. Therefore, it is necessary to investigate a method to monitor and evaluate the host-microbial interaction in drug metabolism.

Previously, the most concerns of the global human gut microbiome related to decoding the whole-genome of all microbes, which have been largely answered by recent advanced techniques. Although host-microbial interactions are indeed important in human metabolism, as well as in drug metabolism, its properties are currently have not been fully understood, mainly due to the limitation of the technology. A directly monitoring method may help shed light on the actual course of metabolic bioprocess and then uncover potentially host-gut microbe interactions. Recent researches showed the method of real-time monitoring metabolism provides a comprehensive time-dependence view to highlight the critical insight of the actual metabolic pathway (27). In particular, the development of real-time NMR recently exhibited new achievements as a potential method for time-dependent observing and quantitatively measuring metabolic activity. By the advantages as a non-destructive and real-time method, it has been already successfully developed and applied on various biological levels such as organelle, whole-cell, whole-organism systems (27-29). Therefore, the real-time course would advance in following comprehensively inter-species interactions, especially host and gut microbiome in the drug metabolism. Then, the contribution of the gut microbiome to human systemic metabolism could be quantitatively and qualitatively evaluated. However, there are still challenges in real-time studying the human microbiome, incredibly functional proof-of-concept study. Here, I investigated the host-gut microbial interaction on a

living whole-body biosystem, *C. elegans.* The host, *C. elegans* with high properties of human homologs genes, presented the similarity of human tissue, and bacterial food source met up with the representative gut microbiome. I focused on developing a real-time NMR method of monitoring and analyzing the host-gut microbial interaction in metabolizing drug of 5-FU to the inactivated formation. This method was exhibited as an applicable method for finding the role of gut microbiota containing homogenous metabolic enzymes in the overall-metabolism of humans.

Materials and Methods

1. **Table 1.** Chemical and Reagents

Chemical and Reagents	Source	Identifier
5-FU	Sigma	Lot. #MKBS2555V
RNeasy Mini Kit (Qiagen)	Qiagen	Lot. #102211153
High Capacity cDNA Reverse Transcription Kit	Applied Biosystems	Lot. #1304185
SYBR Green Supermix	Bio-Rad	Cat. #172-5120
Primers dpyd-1	Bioneer	Forward: GACGCAGTTTTGTCGGCTTT Reverse: AGGCGGCAATCTTTCCATCA
Primers actin-1	Bioneer	Forward: GCTTCAGTGAGGAGGACTGG Reverse: GTCGGTATGGGACAGAAGGA

2. **Table 2. Experimental organisms/strains**

Organisms/strains	Source	Identifier
C. elegans strain N2	Caenorhabditis Genetics Center (CGC)	Wild-type Bristol
E. coli OP50	Caenorhabditis Genetics Center (CGC)	N/A
E. coli JW2133	Dharmacon (GE life sciences)	Ref. #SO-2794270G *E. coli preT/preA* deletion
E. coli K12	KCTC (Korean Collection for Type Culture)	KCTC 1116 Human gut microbe (30)
E. coli MG 1655	KCCM (Korean Culture Center of Microorganisms)	KCCM 41310 Human gut microbe (31)
E. coli HT1115 - RNAi dpyd-1	This study*	*E. coli* HT115 (DE3) containing plasmid L4440 with RNAi *dpyd-1*
E. coli HT1115 - RNAi control	This study*	*E. coli* HT115 (DE3) containing plasmid L4440 control
*Commercial probiotics	Pharm Cross Co., Ltd	Triple premium alive probiotics

**E. coli* HT1115 containing RNAi *dpyd-1* and control are kind gifts from Prof. Junho Lee (Department of Biological Sciences, Institute of Molecular Biology and Genetics, Seoul National University)

** Commercial probiotics product was purchased from Pharm Cross Co., Ltd (㈜팜크로스) as triple premium alive probiotics, including Lactobacillus plantarum, Enterococcus faecium, Bifidobacterium animalis spp. lactics, Lactococcus lactics, Streptococcus thermophiles, Lactobacillus rhamnosus, Lactobacillus acidophilus, Lactobacillus casei, Bifidobacterium breve, Bifidobacterium longum, Lactobacillus paracasei, Bacillus subtilis, Clostridium butyricum strain Miyairi

3. *C. elegans*/gut microbial strains culture:

This study used *C. elegans* wild-type Bristol strain N2 as the host model for drug metabolism. The animals were generally cultured with *E. coli* OP50 as a food source plating on NGM agar following described protocol (32). For synchronizing generation, the bleaching technique was utilized for harvesting eggs from gravid *C. elegans*. The first larval stage (L1) hatching occurred contemporaneously and grew up to the adults stage then (52h).

All bacterial strains were grown in Luria Broth (LB) at 37°C with the assigned selection antibiotics. Laboratory strains were used 100 µg/mL Streptomycin for *E. coli* OP50, 100 µg/mL Kanamycin for *E. coli* JW2113 *preT/preA* deletion (preT/preA KO). *E. coli* HT115 (DE3) containing plasmid L4440 with RNAi *dpyd-1*(RNAi *dpyd-1*) or control (RNAi control) were grown in LB containing 100 µg/mL Ampicillin, then added IPTG to 1mM as described method (33). Human microbial florae *E. coli* MG1655 (KCCM 41313) and *E. coli* K12 (KCTC 1116) were grown in Luria Broth (LB) without supplementary antibiotics. Commercial probiotics were cultivated within LB under both anaerobic and aerobic conditions.

4. Preparation of sample for NMR assessment:

Host-gut microbial system

Synchronized adult *C. elegans* fed with different bacterial strains respectively were collected in M9 buffer and removed bacteria sticking to the *C. elegans*' surfaces by washing method with sucrose 35%(w/v) at 20°C, 2900 g centrifugation in 3 min (34). Approximately 200.000 worms were recruited after washing three times with LB

medium. Animals were treated with 5-FU at a final concentration of 5mM in total 2mL of complex of worms and LB medium contained in 15mL tube and further incubated on a roller drum at 20ºC for 3 hours. After incubation, animals have measured the survival rate by counting moving worms and transferred to NMR tube (27). Notably, worms were accumulated to the stable sediment coverage of the NMR detection region by light centrifugation (100g for 15s), and gently collected supernatant to remain final the 500uL of worms. Afterward, the coaxial insert as external referencing containing 0.005% Trifluoroacetic acid (TFA) in Deuterium (D_2O) was added inside to complete the sample for NMR acquirement. Collected supernatants were also sampled for concurrently NMR measurement.

Gut microbial system

To illustrate the drug-metabolizing possibility of *C. elegans*' gut microbiome system, a drug testing method was establish for normalizing bacterial capacity to be an equivalent total of 20 x 10^8 bacterial cells colonized in the gut of 200.000 worms (35, 36). Bacterial strains were grown in 20mL LB medium at 37ºC, 180rpm in 12h, and recorded OD_{600nm} reaching a range of 0.8-1.0 in log-phage using the spectrophotometer (37). The pellet of bacteria was collected by centrifugation (3000 rpm, 37ºC, 5 min), then diluted with LB medium to reach OD_{600nm} = 1.0, estimating 8 x 10^8 bacterial cells/mL(38). Collection of 20 x 10^8 bacterial cells were obtained in 0.5mL of LB medium containing a final concentration of 5-FU at 5mM and further incubated at 20ºC. After 6h-incubation, the mixed of 500uL bacteria were sampled for NMR measurement

5. 19F-NMR acquirement and data processing:

NMR experiments were performed with JEOL 400MHz NMR Instrument operating by 1D-^{19}F channel with locking phase by D_2O solvent. NMR spectra were obtained at 20ºC using the ^{19}F with the following parameters: transmitter frequency 376.17MHz, spectral width 75.75 kHz, acquired size 65536, pulse width 6.18µs; relaxation delay 1.0s, the number of scans 704, receiver gain 62, acquisition time 20 min/time point (total 9-time points). After NMR acquirement, animals were also imaged and recorded

the survival rate (after).

By using MNOVA software version 9.0.1, taken spectra were transformed (exponential 10Hz), phased, baseline corrected. With coaxial insert, trifluoroacetic acid in D_2O was referenced at 0 ppm and normalized for fluorine-peak integral quantification. The chemical shift of NMR peaks was assigned according to the previous study (Table 3) (39). The integral of sequential NMR peaks were exhibited as area graphs and computed the area under the curve (AUC) for all time points

6. Phenotypic classification of *C. elegans* in response to chemotherapy

The effect of different bacterial strains containing a 5-FU catabolic homogenous enzyme system on the host was evaluated by the response to phenotypic development. 5-FU was diluted in NGM agar in a 48-well plate following serial final concentrations 0, 2.5, 5, 10, 20, 40, 80, 160 uM, respectively. 20uL of *E. coli* overnight culture was collected and resuspended in fresh LB to reach OD_{600nm} = 2.0. Then 50uL of cultures was added on NGM agar containing the drug. Approximately 50-100 synchronized L1 stage *C. elegans* in M9 buffer were seeded on NGM agar prepared above. Animals were grown in the incubator at 20ºC for 60 hours when the animals reached the gravid adult stage. The phenotype of *C. elegans* with different gut microbial strains in response to 5-FU treatment was observed at 4X magnification by a microscope, captured by Scope Camera, and classified by the criteria following:

- Developed (Adults and L4 stage)
- Delayed (L3 and L2 stage)
- Arrested (L1 stage and death)

(Compared with the control sample without drug treatment)

7. Quantification of mRNA expression level

After the NMR experiment, the *C. elegans* fed with *E. coli* containing RNAi *dpyd-1* or control were recruited to measure the level of dpyd-1 expression. Approximately 1000 nematodes were washed with M9 medium and collected pellet in EP tube. Following the manufacturer-recommended protocol, total RNA was isolated using the RNeasy

Mini Kit (Qiagen). After quantitatively and qualitatively analyzing purified RNA using NanoDrop (Thermo Scientific), 2µg RNA was utilized to synthesize cDNA using the High Capacity cDNA Reverse Transcription Kit. Real-time PCR was performed using SYBR Green Supermix. The *C. elegans*' primers targeting gene *dpyd-1* (Forward: GACGCAGTTTTGTCGGCTTT and Reverse: AGGCGGCAATCTTTCCATCA) were used for qRT-PCR analysis. The ΔΔCt values were calculated representative to gene expression, which normalized to the expression of housekeeping gene actin-1 (Forward:GCTTCAGTGAGGAGGACTGG and Reverse: GTCGGTATGGGACAGAAGGA)

8. Data analysis:

GraphPad Prism version 9.1.1 was in use to exhibit the graphs. Triplicated data were gathered and analyzed together. The area under the curve (A.U.C) and gene expression levels are presented as the mean ± standard error of the mean (SEM), and statistical analyses by using Student's t-test indicated $p^* < 0.05$ as a significant difference.

III. Results

A. Establishment of ^{19}F-NMR for real-time observing the drug catabolism in the host-gut microbial system

For this study, ^{19}F-NMR was established and applied on *in vivo* system of *C. elegans* fed with bacteria for real-time monitoring of 5-FU metabolism. In particular, *C. elegans* (host) and *E. coli OP50* (gut microbiome) were representative of inter-species biological system in drug (5-FU) metabolism *in vivo*. The schematic of the experimental setup for real-time observing the drug catabolism in the host-gut microbial system was shown in Figure 1. Approximately 200,000 live adult worms after 3h-treatment of 5-FU were transferred to standard NMR tube with 3 mm coaxial insert containing 0.005% TFA in D_2O, and real-time monitored in 3h-acquisition by using ^{19}F-NMR then. As a fluorinated-pyrimidine antagonist, the schematic catabolic pathway of 5-FU in humans was shown in Figure 2 following previous studies (40, 41). The process of 5-FU catabolism exhibits three main sequential stages to produce three primary inactivated metabolites including 5-*Fluorodihydrouracil* (FUH_2), *α-fluoro-ureidopropionic acid* (FUPA), and *Fluoro-β-alanine* (FBAL) (Figure 2). These metabolites representing the catabolic activity of 5-FU in the host-gut microbial system was real-time monitored by 19F-NMR and exhibited by sequential spectrum in 3h- acquisition. The continuous trend in the decay of 5-FU signal and the increase of catabolites (FUPA, FBAL) demonstrated that the 5-FU catabolism clearly occurred in incubation time and continued following the time of NMR measurement (Figure 3). Figure 4 showed the absence of these metabolites in the supernatant after the experiment metabolism, which confirm the processing catabolism that occurred within *C. elegans*. In addition, the method also included the relevance to physiological metabolism of living animals by evaluating the survival rate before and after NMR measurement. The higher 95% of moving worms as survival rate after experiment indicated the

living property of animals during the measurements, or the live metabolomics method (Figure 4).

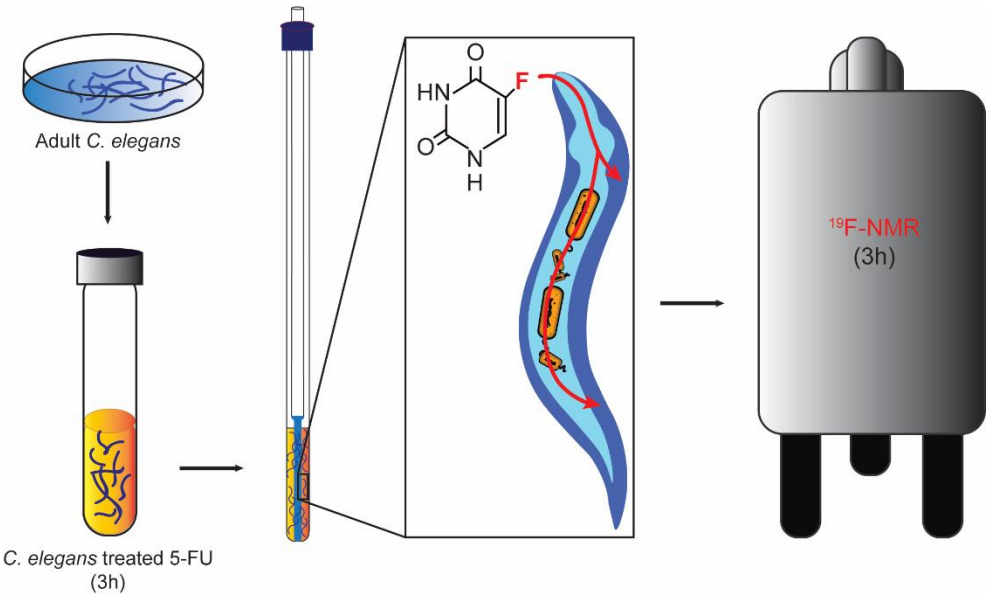

Figure 1. Overall schematics for real-time observation of the host-gut microbial interspecies interaction in anticancer drug (5-FU) metabolism.

C. elegans were grown in agar plates with *E. coli* to the adult stage (L4), harvested, and then incubated with 5-FU in liquid culture. The worms were then moved to a standard NMR tube to monitor 5-FU catabolism within the living biological system of *C. elegans* fed with *E. coli*.

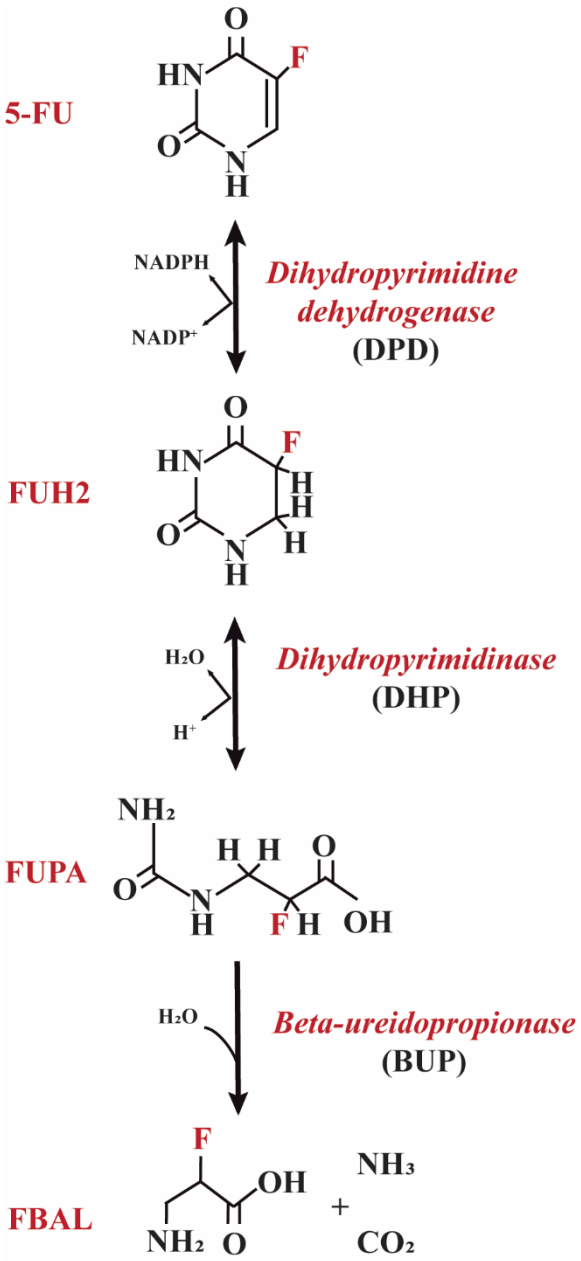

Figure 2. Schematic representation of general 5-FU catabolism into its main products (42). 5-fluorouracil (5-FU), α-fluoro-ureidopropionic acid (FUPA), fluoro-β-alanine (FBAL), dihydropyrimidine dehydrogenase (DPD), dihydropyrimdinase (DPYS), and β-ureidopropionase (BUP)

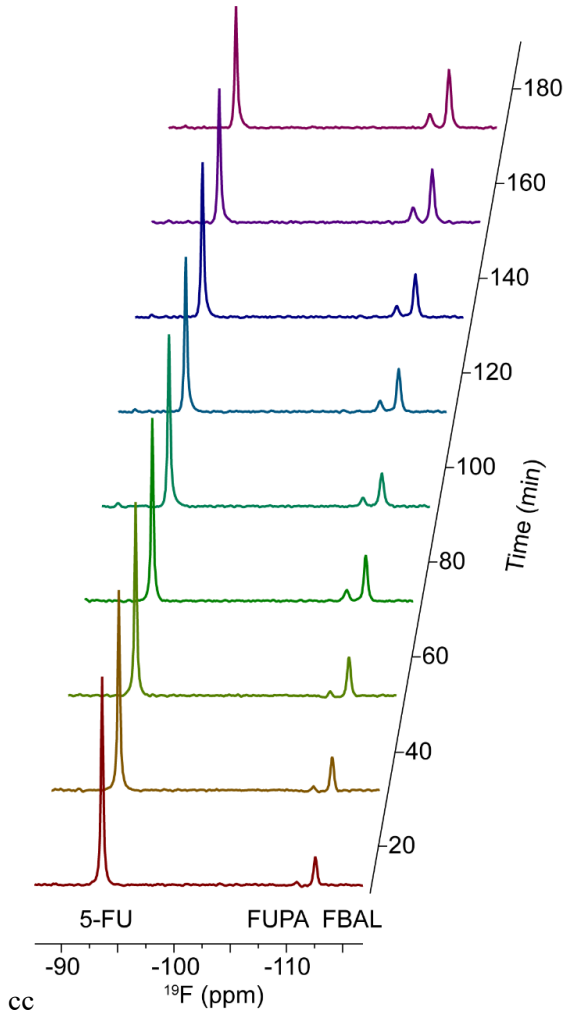

cc

Figure 3. Overlay of sequential 1D ^{19}F-NMR spectra of the living host-gut microbiome system showing time-dependent 5-FU catabolism and the concomitant production of its catabolites.

Spectra were taken at 20°C by a JOVE 400MHz NMR with the following parameters: transmitter frequency 376.17MHz, spectral width 75.75 kHz, acquired size 65536, pulse width 6.18μs; relaxation delay 1.0s, the number of scans 704, receiver gain 62, acquisition time 20 min/time point (total 9 time points). 5-fluorouracil (5-FU), α-fluoro-ureidopropionic acid (FUPA), fluoro-β-alanine (FBAL). Assignment of peaks were obtained by spiking with signal to external standard TFA at δ = 0 ppm, see Table 3.

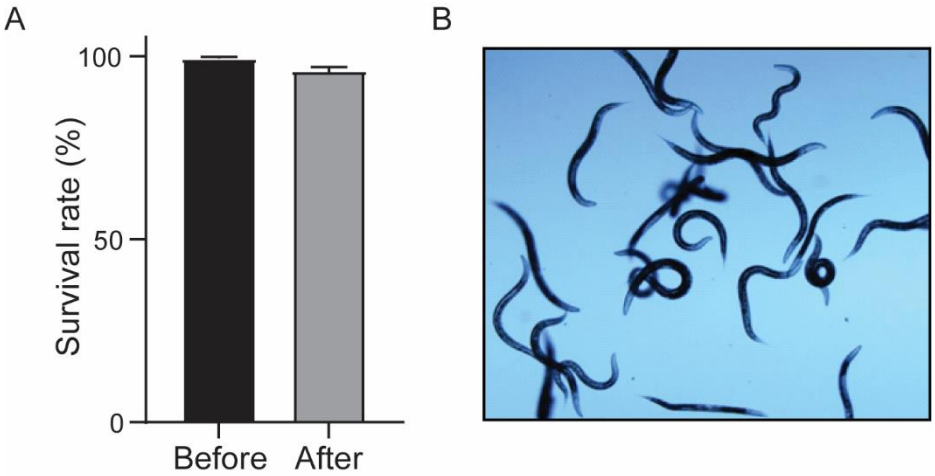

Figure 4. The feasibility of studying live worms for *in vivo* model

A: The survival rate of worms before and after NMR measurement by counting the moving worms. Error bars represent the standard deviations from three independent experiments.

B: Visualization of living worms under the microscope after 3h of NMR measurement

No.	METABOLITE	Abbreviation	^{19}F
1	5-fluorouracil	5-FU	−93.6
2	Dihydro-5-fluorouracil	FUH_2	−125.8
3	α-fluoro-ureidopropionic acid	FUPA	−110.8
4	Fluoro-β-alanine	FBAL	−112.5
5	Trifluoroacetic acid	CF3COOH	0

Table 3. Metabolites identified by spiking with reference signal to external standard TFA at δ = 0 ppm

No.	Enzyme	Abbreviation	Gene
1	*Dihydropyrimidine dehydrogenase*	DPD	DPYD
2	*Dihydropyrimidinase*	DHP	DPYS
3	*β-ureidopropionase*	BUP	BUP1

Table 4. Catabolic enzymatic system of pyrimidine catabolism in human

B. Drug catabolic activity in separation of the host versus gut microbiome

The above results come from the biological model contains the host and microbiome, therefore, we separated the catabolic activity on the host and gut microbiome, separately. For gut microbiome, hereby, we investigated 5-FU catabolic activity on *E. coli* OP50, which strain had been studied in drug-resistence in *C. elegans*. Consistently, the peak of FUH2, an intermediate catabolites of 5-FU catabolic cascade, was obtained at -125.8 ppm from the ^{19}F-NMR measurement of *E. coli OP50* treated with 5-FU after 6h incubation. This result suggested OP50 may interfere to the general catabolism of 5-FU on inter-species *C. elegans* – gut microbiome system by contributing an intermediate catabolite, FUH_2. In addition, *preT/preA* in *E. coli* – the ortholog of human DPD, played role in first step of generating 5-FU to FUH_2, were reported in previous studies. Therefore, we experimented 5-FU catabolic activity on *E. coli JW2113 preT/preA* deletion (preT/preA KO), there is no downstream catabolic production of 5-FU obtained on ^{19}F-NMR spectrum (Figure 5). Therefore, *preT/preA* KO *E. coli* could be in use as the gut microbiome of *C. elegans*, as well as an applicable model for separating the catabolism of 5-FU for the host-only.

For the *C. elegans*, pyrimidine catabolism-related orthologs including dpyd-1, dph-2, and upb-1 are responsible for 5-FU degradation. By taking advantage of the *preT/preA KO E. coli*, the obtained catabolism of 5-FU on host-only was showed on Figure 6. The real-time peaks of FUPA, and FBAL were detected, therefore, this results indicated that the host also contains a itself enzyme system of 5-FU catabolism. To more proven, a strain of *E. coli* HT115 was developed as a carrier of RNAi dpyd-1 to knockdown the expression of DPYD in host. For only gut microbiome, *E. coli* HT115 containing RNAi dpyd-1 and RNAi control both catabolize 5-FU to FUH_2, did not exhibit any significant difference in 5-FU catabolism (Figure 7). Moreover, by using HT115 *E. coli* containing RNAi dpyd-1,

the expression level of DPYD on the host is significant reduced (Figure 2D), and lowered consistently catabolic level of 5-FU as evidence of decreased trend of FBAL in real-time observation (Figure?) comparing to the control.

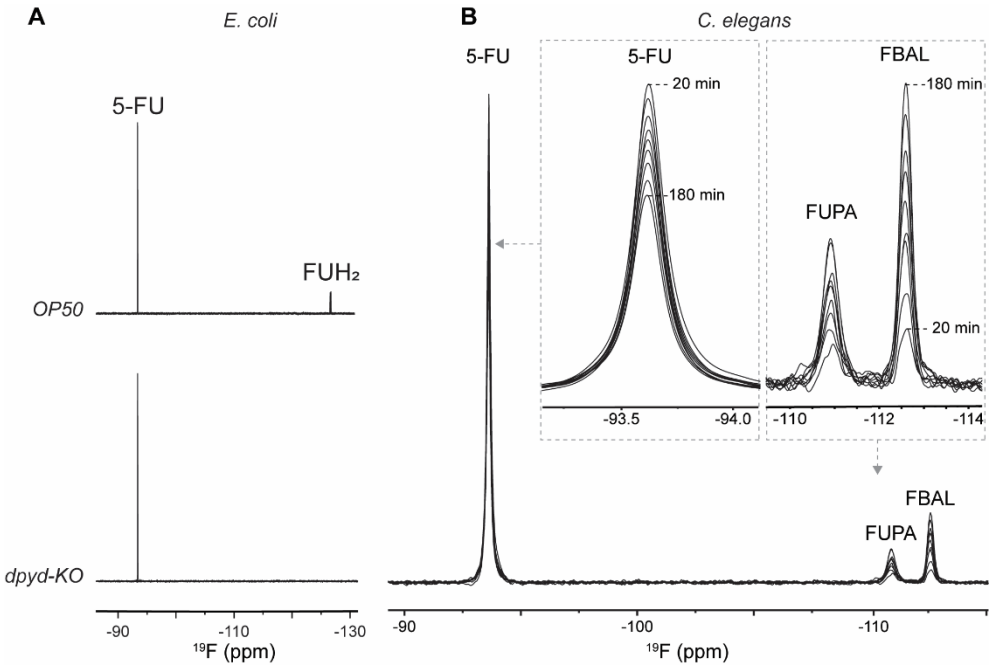

Figure 5. Separation of 5-FU catabolism between gut microbiome and the host

A: ^{19}F-NMR spectra for the catabolism of 5-FU by *wild-type OP50* (upper) or *preT/preA KO E. coli* (lower).

B: Overlay of real-time 19F-NMR spectra for 5-FU catabolism acquired from live *C. elegans* fed with *preT/preA KO E. coli*.

Spectra were taken at 20ºC by a JOVE 400MHz NMR with following parameters: transmitter frequency 376.17MHz, spectral width 75.75 kHz, acquired size 65536, pulse width 6.18μs; relaxation delay 1.0s, the number of scans 704, receiver gain 62, acquisition time 20 min/time point (total 9 time points). 5-fluorouracil (5-FU), α-fluoro-ureidopropionic acid (FUPA), fluoro-β-alanine (FBAL). Assignment of peaks were obtained by spiking with signal to external standard TFA at δ = 0 ppm, see Table 3.

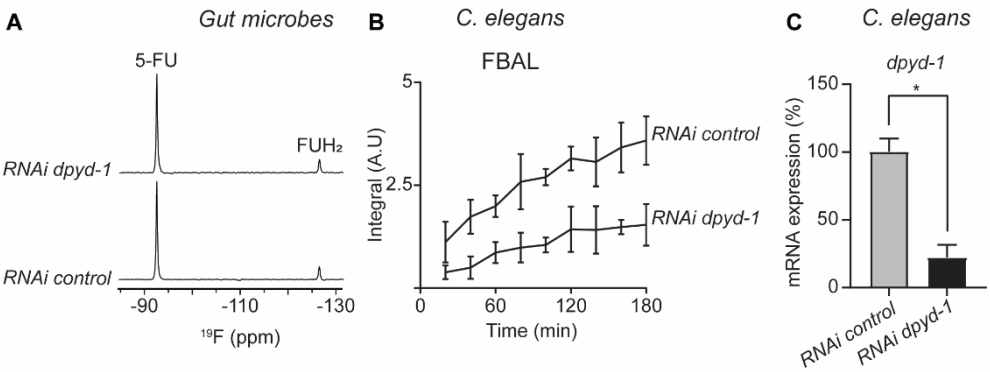

Figure 6. Drug catabolic activity on the host knockdown the expression of dpyd-1

A: ^{19}F-NMR spectra for the catabolism of 5-FU by *E. coli* used as gut microbiome. Upper: *E. coli* containing siRNA for dpyd-1; Lower: *E. coli* with the control vector. Spectra were taken at 20ºC by a JOVE 400MHz NMR with following parameters: transmitter frequency 376.17MHz, spectral width 75.75 kHz, acquired size 65536, pulse width 6.18μs; relaxation delay 1.0s, the number of scans 704, receiver gain 62, acquisition time 20 min/time point (total 9 time points). 5-fluorouracil (5-FU), α-fluoro-ureidopropionic acid (FUPA), fluoro-β-alanine (FBAL). Assignment of peaks were obtained by spiking with signal to external standard TFA at $\delta = 0$ ppm, see Table 3.

B: Real-time catabolic activity of 5-FU in *C. elegans* fed with *E. coli* containing either RNAi dpyd-1 nor RNAi control. The data points was retrived from integral of NMR peaks

C: Gene expression of dpyd-1 in *C. elegans* fed with control or siRNA *E. coli*, as measured with RT-PCR. * represents $p < 0.05$ by student's t-test.

Error bars represent the standard deviations from three independent experiments.

C. Host-gut microbial interaction in drug metabolism

Above all, *C. elegans* were used as the host, and can catabolize 5-FU fully following the 5-FU catabolic cascade to FBAL. Moreover, *E. coli* OP50 played role as the *C. elegans*'s gut microbiome, and could enter to the first and the most important step of 5-FU catabolic cascade by generating to FUH2. By this way, *E. coli* OP50 could contribute to the general catabolism of 5-FU on the inter-species system. In the other hand, by spiking the integral of catabolite peaks, we could quantitative analysis the catabolic level of 5-FU in only host and the host-gut microbial system. Figure 6 showed the significant different level of 5-FU catabolites (FBAL) following time of NMR measurement between only host and the host-gut microbial system. The gap level of FBAL compared *C. elegans* fed with *E. coli* OP50 to the host-only (fed with preT/preA KO) indicated the contribution of gut microbiome to the host metabolism as the inter-species interaction. From this, we could obtain quantitative contributions of 5-FU metabolism, by measuring the area under the curve of the time courses. It turned out that the gut microbiome contributed about 30% to the total 5-FU catabolism of the symbiotic system by providing FUH2. Therefore, the method of ^{19}F-NMR has been successfully established to monitor host-gut microbial interaction in 5-FU catabolism

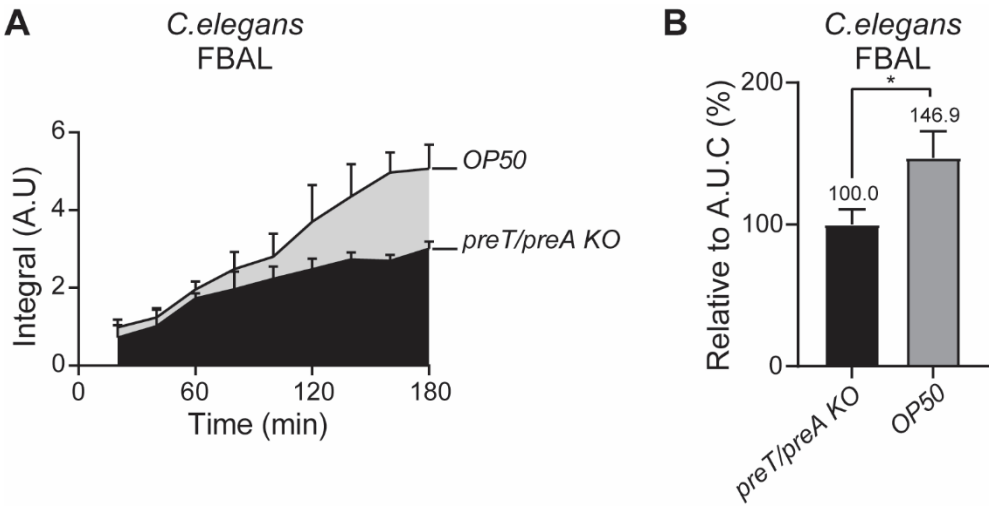

Figure 7: Elucidation of the host-gut microbial interaction in drug metabolism

A: Real-time evaluation of the host-gut microbial interaction in drug metabolism. The values are derived from the integrals of the ^{19}F-NMR spectrum, referred to as the concentration final catabolic production, FBAL. The integral is for FBAL from the spectra in Figure 3 and Figure 5B.

B: Quantification of the contribution of the gut microbiome to the 5-FU catabolism on the host. AUC value obtained from (A) normalized (100%) to that for the *preT/preA*-KO *E. coli* group. The difference between the two groups represents the quantitative contribution from gut microbiome to the 5-FU catabolism on the host. * represents $p < 0.05$ by student's t-test

Error bars represent the standard deviations from three independent experiments.

D. Elucidate the potential of human gut microbes on drug metabolism

We proposed that method can be applied to human bacterial level, therefore, strain of human commensal microbe *E. coli* MG1655, *E. coli* KCTC116 (30) and commercial probiotics. Probiotic bacteria were grown up in LB medium and tested with 5-FU, we could not obtain any catabolites peak on ^{19}F-NMR spectrum. However, *E. coli* KCTC116 could catabolize 5-FU to FUH2, and also FBAL. Interestingly, by OD600-normalization of bacterial number, the level of 5-FU catabolism on *E. coli* KCTC1116 was higher than *E. coli* OP50 (Figure 4B). This predicts the possibility of *E. coli* KCTC116 to participate in general 5-FU catabolism on host-gut microbial system more than *E. coli* OP50.

Consistently, by applying method on *C. elegans* fed with *E. coli* KO-dpyd, *E. coli* OP50, and *E. coli* KCTC1116, respectively, the levels of 5-FU catabolism obtained by accumulation of catabolites were significantly different. *E. coli* KCTC containing two homogenous metabolic enzymes could highest leveled up the 5-FU catabolism on biological system compare *E. coli* OP50 and *E. coli* KO-dpyd. That means in the context of large abundance of human microbiota containing homogenous metabolic enzymes, they may contribute to drug metabolism, or human metabolism in general. Our method worked on both lab bacteria, and human gut bacteria, exhibited an applicable method for valuation the contribution of gut microbiome to host metabolism

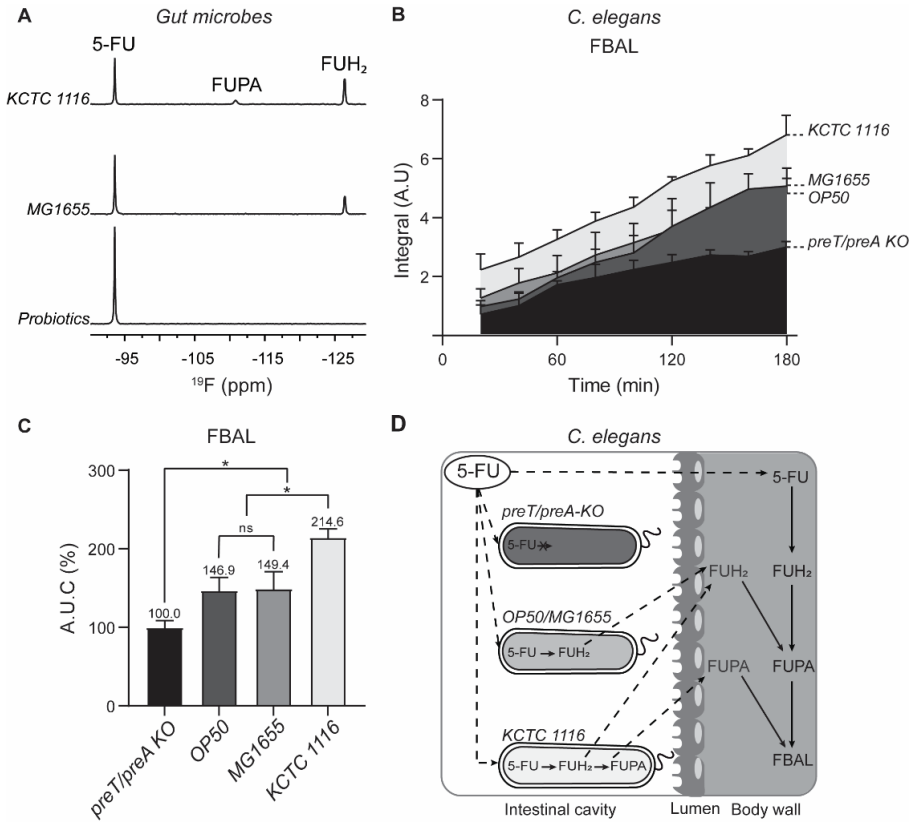

Figure 8: The roles of human gut microme on host (*C. elegans*) 5-FU catabolism

A: Real-time catabolic activity of 5-FU in *C. elegans* (host) fed with KCTC1116 (human gut microbiota) or OP50 (laboratory bacteria) *E. coli* or a commercial probiotics. The integrals are for FBAL from the real-time 19-F NMR spectra.

B: Real-time catabolic activity of 5-FU in *C. elegans* (host) fed with KCTC1116 (human gut microbiota) or *OP50* (laboratory bacteria) *E. coli* or a commercial probiotics. The integrals are for FBAL from the real-time 19-F NMR spectra.

C: AUC values obtained from (B) normalized (100%) to that for the *preT/preA*-KO *E. coli* group. The differences between the groups represent the quantitative contribution from gut microbiome to the 5-FU catabolism on the host.

D: Schematics of the inter-species interaction in the host- gut microbial system for the catabolism of 5-FU with bacteria containing different metabolic genes.

E. The translation of gut microbial contribution to drug metabolism into phenotypic development of the host

To further confirmation the inter-species interaction in drug metabolism, we investigated a long-term observation the phenotypic development of the host fed with different bacterial strains in response to 5-FU treatment. In general, the developmental phenotype of *C. elegans* were exhibited different level following the increasing 5-FU concentrations, and according to the different feeding bacterial strains (Figure 9A). The phenotypes were identified as the category in Figure 9B, and presented in a tabular representation in Figure 9C. The toxicity was highest, with the developmental arrest at the lowest 5-FU concentration, for the worms fed with the microbiome having the smallest contribution to the 5-FU catabolism (preT/preA KO) and was lowest for those fed with KCTC1116 having the highest catabolic contribution. This shows that the level of 5-FU catabolism by gut microbiome, as measured with our real-time approach, significantly reduced the drug toxicity in *C. elegans* development.

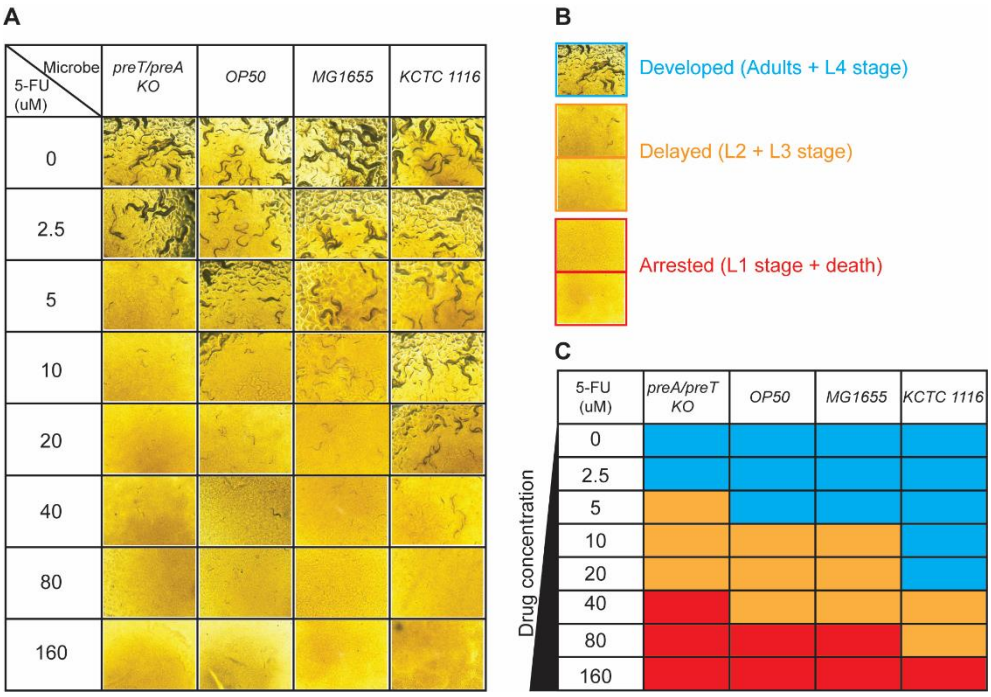

Figure 9. Effects of gut microbiome on the differential toxicity of 5-FU to *C. elegans* host

A: Concentration dependent effects of 5-FU on the *C. elegans* development according to different gut microbiome.

B: Representative developmental stages of *C. elegans* growing on different 5-FU concentrations. Blue: Developed; Yellow: Delayed, Red: Arrested.

C: A tabular representation of (A) using the color scheme of (B)

DISCUSSION

The NMR have been widely studied in metabolism and taken advantages on various model levels from in-organelle to whole-body system (27, 29). Hereby, we would like to develop a real-time NMR method forwarding to study metabolism on up-grade interspecies level. Therefore, the interaction between host and gut microbiome in drug metabolism was the main strategy for this study. We employed real-time ^{19}F-NMR as a novel visualization and quantitative method of the inter-species metabolic interaction in the present study. Particularly, we recruited *in vivo* system of *C. elegans* fed with *E. coli OP50 as the host-gut microbial model* for real-time monitoring of 5-FU catabolism (Figure 1). The method had been successfully established, ^{19}F-NMR directly illustrated the fundamental performance for real-time change of 5-FU and its catabolites (FUPA, FBAL) accumulation in a living system, *C. elegans* fed with bacteria (Figure 3). The physiological integrity of the experimental model was shown by the animal morphology and survival rate after the experiment over than 95% (Figure 4), which was commensurate to previous research on *in vivo C. elegans* model. In addition, by washing method with sucrose 35% mentioned in the method, we confirmed that the metabolism occurs within *C. elegans* by showing the absence of these metabolites in the supernatant after the experiment (Figure 10)

In biomedicine, *C. elegans* is widely chosen as a potential model organism to laboratory and precinical experiments about human diseases such as neuronal, cardiovascular, muscular, tumorous, aging diseases because of counterparts for many homologs human genes (80%). Especially, *C. elegans* is ideally used *in vivo* testing for anticancer drugs (43). Currently, class of fluorine-containing pharmaceuticals is gradually increasing number of discovery drugs in cancer treatment. Therefore, the metabolism of fluorine-containing drug in biological system is essential for clinical application in the future, and this developed real-time ^{19}F-NMR is really a promising method. In addition, ^{19}F-NMR has been well-known as a highly powerful technique

for determining the biological accumulation of fluorine containing molecules in living biological system. By providing the ^{19}F-NMR spectrum, signals of metabolites are usually resulted in their specific chemical shifts without background interference. Therefore, monitoring the fluctuations of fluorine-chemical accumulation in the host-microbial system indicated not only the changing level of metabolites but also showed feasibility for quantitative delineation of drug metabolism on biological system.

In this study, the host (*C. elegans*) and gut microbiome (OP50) cooperatively generated 5-FU following the catabolic cascade. Therefore, we separated the catabolism of 5-FU on the host-only and gut microbiome by using a bacterial strain deletion preA/preT (DPD orthologs) as the first enzyme of 5-FU catabolic pathway. This *E. coli* strain does not appreciable activities in 5-FU catabolism with any visible peak from ^{19}F-NMR spectrum. This study functionally proved that the preT/preA, the suggested DPYD ortholog, is actually responsible for the generation of FUH2 in *E. coli* as a gene-metabolic activity relationship. Taking advantages of preT/preA *E. coli*, we quantified the contribution of gut microbiome to contribute to the overall 5-FU catabolism (Figure 7). This is the novelty of the method for the assessment, and also represents the inter-species interactions in overall drug metabolism in biological systems.

So far, to show the relevance of our approach for human gut microbiome, we tested it with bacterial species with implications in human health. We tried other *E. coli* strains that are members of human gut microbiome: KCTC 1116, MG1655 and commercial probiotics. Surprisingly, these bacteria showed surprising differences in 5-FU catabolism. Probiotics cultivated in both anaerobic and aerobic conditions, could not catabolize 5-FU. However, 5-FU was generated in the first step with MG1655, and up to second step with KCTC 1116 following catabolic cascade. This means different bacterial species containing homogenous enzyme have their own ability in drug metabolism, respectively. Then, we also investigated the difference in

general 5-FU catabolism of *C. elegans* effected by individual symbiotic gut bacteria. Consistently, the overall drug catabolism was obtained in significant dissimilar level according to the contribution of each gut microbes. Further, the consistence in results of *C. elegans* phenotype classification after long-term expose with 5-FU strongly proved the indication of gut microbiome playing important role in drug metabolism of host-gut microbial system. Therefore, with a large number of species and number cells in the human gut, this finding indicated high-potential human gut microbiome could contribute to not only drug but also the systemic metabolism. The above method lays the groundwork for the assessment of a single or population of human gut microbiome in drug metabolism. And, it is a method that can comprehensively and in detail evaluate the ability of gut microbiome in drug metabolism and in the interaction between gut microbiome and host (46). Moreover, the study also laid the foundation and groundwork for the development of bacteriatherapy in the future, which has been focusing of research and shows great promise in cancer treatment.

In conclusion, we successfully developed real-time 19F-NMR for monitoring the interspecies interaction (host – gut microbiome) in the metabolism of Fluorine-containing drug (5-FU) on biological system (*C. elegans*). The applicable method for finding role and quantitative estimation the contribution of gut microbiota containing homogenous metabolic enzymes in overall-metabolism of the host. Moreover, the method given properties to extend the findings on other anticancer drugs, bacterial species, and NMR-specific channels on *C. elegans* with metabolic implications.

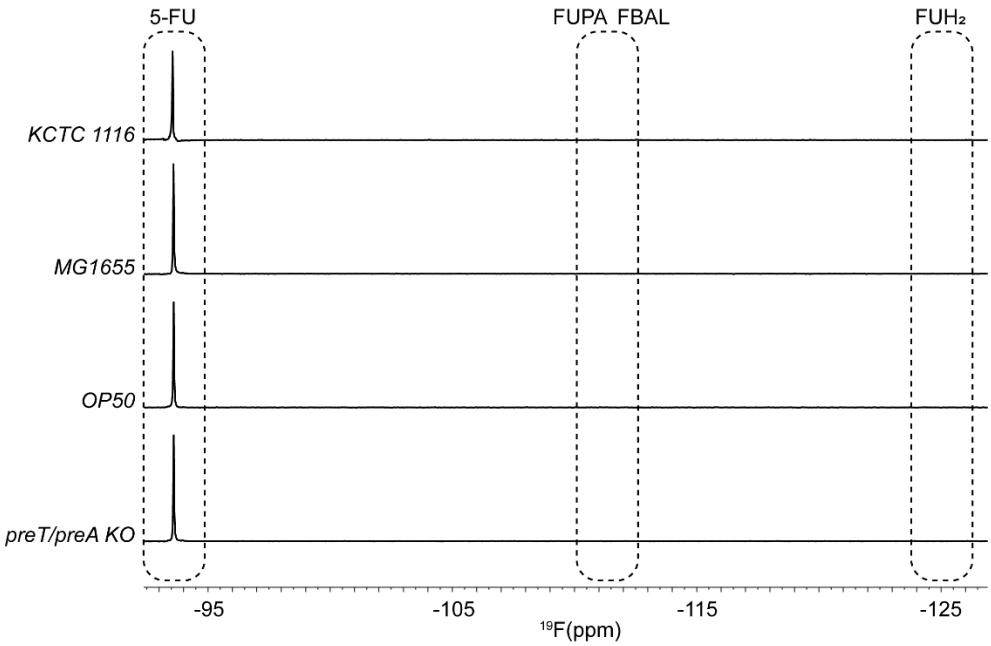

Figure 4. ^{19}F-NMR spectrum of supernatant obtained from host-gut microbial samples (Fig. 3B) after 3h-incubation with 5-FU.

Spectra were taken at 20°C by a JOVE 400MHz NMR with following parameters: transmitter frequency 376.17MHz, spectral width 75.75 kHz, acquired size 65536, pulse width 6.18μs; relaxation delay 1.0s, the number of scans 704, receiver gain 62, acquisition time 20 min/time point (total 9 time points). 5-fluorouracil (5-FU), α-fluoro-ureidopropionic acid (FUPA), fluoro-β-alanine (FBAL). Assignment of peaks were obtained by spiking with signal to external standard TFA at δ = 0 ppm, see Table 3.

REFFERENCES:

1. Marchesi JR, Ravel J. The vocabulary of microbiome research: a proposal. Microbiome. 2015;3:31.

2. Lederberg J, McCray AT. `Ome Sweet `Omics--A Genealogical Treasury of Words. The Scientist. 2001 2001/04/02/:8.

3. Huang X, Fan X, Ying J, Chen S. Emerging trends and research foci in gastrointestinal microbiome. J Transl Med. 2019;17(1):67.

4. Lynch SV, Pedersen O. The Human Intestinal Microbiome in Health and Disease. New Engl J Med. 2016;375(24):2369-79.

5. Turnbaugh PJ, Ley RE, Hamady M, Fraser-Liggett CM, Knight R, Gordon JI. The human microbiome project. Nature. 2007;449(7164):804-10.

6. Sender R, Fuchs S, Milo R. Revised Estimates for the Number of Human and Bacteria Cells in the Body. PLoS Biol. 2016;14(8):e1002533.

7. Yassour M, Vatanen T, Siljander H, Hamalainen AM, Harkonen T, Ryhanen SJ, et al. Natural history of the infant gut microbiome and impact of antibiotic treatment on bacterial strain diversity and stability. Sci Transl Med. 2016;8(343):343ra81.

8. Goodrich JK, Waters JL, Poole AC, Sutter JL, Koren O, Blekhman R, et al. Human genetics shape the gut microbiome. Cell. 2014;159(4):789-99.

9. Rothschild D, Weissbrod O, Barkan E, Kurilshikov A, Korem T, Zeevi D, et al. Environment dominates over host genetics in shaping human gut microbiota. Nature. 2018;555(7695):210-5.

10. Thaiss CA, Zeevi D, Levy M, Zilberman-Schapira G, Suez J, Tengeler AC, et al. Transkingdom control of microbiota diurnal oscillations promotes metabolic homeostasis. Cell. 2014;159(3):514-29.

11. Claesson MJ, Jeffery IB, Conde S, Power SE, O'Connor EM, Cusack S, et al. Gut microbiota composition correlates with diet and health in the elderly. Nature. 2012;488(7410):178-84.

12. Redondo-Useros N, Nova E, Gonzalez-Zancada N, Diaz LE, Gomez-Martinez S, Marcos A. Microbiota and Lifestyle: A Special Focus on Diet. Nutrients. 2020;12(6).

13. Gordon JI. Honor thy gut symbionts redux. Science. 2012;336(6086):1251-3.

14. Maynard CL, Elson CO, Hatton RD, Weaver CT. Reciprocal interactions of the intestinal microbiota and immune system. Nature. 2012;489(7415):231-41.

15. Johansson ME, Jakobsson HE, Holmen-Larsson J, Schutte A, Ermund A, Rodriguez-Pineiro AM, et al. Normalization of Host Intestinal Mucus Layers Requires Long-Term Microbial Colonization. Cell Host Microbe. 2015;18(5):582-92.

16. Petersson J, Schreiber O, Hansson GC, Gendler SJ, Velcich A, Lundberg JO, et al. Importance and regulation of the colonic mucus barrier in a mouse model of colitis. Am J Physiol Gastrointest Liver Physiol. 2011;300(2):G327-33.

17. Morowitz MJ, Carlisle EM, Alverdy JC. Contributions of intestinal bacteria to nutrition and metabolism in the critically ill. Surg Clin North Am. 2011;91(4):771-85, viii.

18. Deehan EC, Duar RM, Armet AM, Perez-Munoz ME, Jin M, Walter J. Modulation of the Gastrointestinal Microbiome with Nondigestible Fermentable Carbohydrates To Improve Human Health. Microbiol Spectr. 2017;5(5).

19. Pascale A, Marchesi N, Marelli C, Coppola A, Luzi L, Govoni S, et al. Microbiota and metabolic diseases. Endocrine. 2018;61(3):357-71.

20. Wang W, Yang Q, Sun Z, Chen X, Yang C, Ma X. Editorial: Advance of Interactions Between Exogenous Natural Bioactive Peptides and Intestinal Barrier and Immune Responses. Curr Protein Pept Sci. 2015;16(7):574-5.

21. Wilson ID, Nicholson JK. Gut microbiome interactions with drug metabolism, efficacy, and toxicity. Transl Res. 2017;179:204-22.

22. Wallace BD, Wang H, Lane KT, Scott JE, Orans J, Koo JS, et al. Alleviating

cancer drug toxicity by inhibiting a bacterial enzyme. Science. 2010;330(6005):831-5.

23. Liang X, Bittinger K, Li X, Abernethy DR, Bushman FD, FitzGerald GA. Bidirectional interactions between indomethacin and the murine intestinal microbiota. Elife. 2015;4:e08973.

24. Meinl W, Sczesny S, Brigelius-Flohe R, Blaut M, Glatt H. Impact of gut microbiota on intestinal and hepatic levels of phase 2 xenobiotic-metabolizing enzymes in the rat. Drug Metab Dispos. 2009;37(6):1179-86.

25. Zimmermann M, Zimmermann-Kogadeeva M, Wegmann R, Goodman AL. Mapping human microbiome drug metabolism by gut bacteria and their genes. Nature. 2019;570(7762):462-7.

26. Javdan B, Lopez JG, Chankhamjon P, Lee YJ, Hull R, Wu Q, et al. Personalized Mapping of Drug Metabolism by the Human Gut Microbiome. Cell. 2020;181(7):1661-79 e22.

27. Nguyen TTM, An YJ, Cha JW, Ko YJ, Lee H, Chung CH, et al. Real-Time In-Organism NMR Metabolomics Reveals Different Roles of AMP-Activated Protein Kinase Catalytic Subunits. Anal Chem. 2020;92(11):7382-7.

28. Xu WJ, Wen H, Kim HS, Ko YJ, Dong SM, Park IS, et al. Observation of acetyl phosphate formation in mammalian mitochondria using real-time in-organelle NMR metabolomics. Proc Natl Acad Sci U S A. 2018;115(16):4152-7.

29. Wen H, An YJ, Xu WJ, Kang KW, Park S. Real-time monitoring of cancer cell metabolism and effects of an anticancer agent using 2D in-cell NMR spectroscopy. Angew Chem Int Ed Engl. 2015;54(18):5374-7.

30. Shin JH, Nam SW, Kim JT, Yoon JB, Bang WG, Roe IH. Identification of immunodominant Helicobacter pylori proteins with reactivity to H. pylori-specific egg-yolk immunoglobulin. J Med Microbiol. 2003;52(Pt 3):217-22.

31. Maltby R, Leatham-Jensen MP, Gibson T, Cohen PS, Conway T. Nutritional basis for colonization resistance by human commensal Escherichia coli

strains HS and Nissle 1917 against *E. coli* O157:H7 in the mouse intestine. PLoS One. 2013;8(1):e53957.

32. Brenner S. The genetics of Caenorhabditis elegans. Genetics. 1974;77(1):71-94.

33. Timmons L, Court DL, Fire A. Ingestion of bacterially expressed dsRNAs can produce specific and potent genetic interference in Caenorhabditis elegans. Gene. 2001;263(1-2):103-12.

34. Foll RL, Pleyers A, Lewandovski GJ, Wermter C, Hegemann V, Paul RJ. Anaerobiosis in the nematode Caenorhabditis elegans. Comp Biochem Physiol B Biochem Mol Biol. 1999;124(3):269-80.

35. Cabreiro F, Gems D. Worms need microbes too: microbiota, health and aging in Caenorhabditis elegans. EMBO Mol Med. 2013;5(9):1300-10.

36. Garsin DA, Sifri CD, Mylonakis E, Qin X, Singh KV, Murray BE, et al. A simple model host for identifying Gram-positive virulence factors. Proc Natl Acad Sci U S A. 2001;98(19):10892-7.

37. Kobayashi A, Hirakawa H, Hirata T, Nishino K, Yamaguchi A. Growth phase-dependent expression of drug exporters in Escherichia coli and its contribution to drug tolerance. J Bacteriol. 2006;188(16):5693-703.

38. Gangan MS, Athale CA. Threshold effect of growth rate on population variability of Escherichia coli cell lengths. R Soc Open Sci. 2017;4(2):160417.

39. Novak MMA, Shimizu K, Blackburn BJ. A fluorine-19 nuclear magnetic resonance study of 5-fluorouracil metabolism in Mesocestoides corti tetrathyridia. Canadian Journal of Zoology. 1992;70(2):406-10.

40. Scott TA, Quintaneiro LM, Norvaisas P, Lui PP, Wilson MP, Leung KY, et al. Host-Microbe Co-metabolism Dictates Cancer Drug Efficacy in *C. elegans*. Cell. 2017;169(3):442-56 e18.

41. Garcia-Gonzalez AP, Ritter AD, Shrestha S, Andersen EC, Yilmaz LS, Walhout AJM. Bacterial Metabolism Affects the *C. elegans* Response to Cancer

Chemotherapeutics. Cell. 2017;169(3):431-41 e8.

42. Mukherjee KL, Heidelberger C. Studies on fluorinated pyrimidines. IX. The degradation of 5-fluorouracil-6-C14. J Biol Chem. 1960;235:433-7.

43. Kobet RA, Pan X, Zhang B, Pak SC, Asch AS, Lee MH. Caenorhabditis elegans: A Model System for Anti-Cancer Drug Discovery and Therapeutic Target Identification. Biomol Ther (Seoul). 2014;22(5):371-83.

44. Stevens AN, Morris PG, Iles RA, Sheldon PW, Griffiths JR. 5-fluorouracil metabolism monitored *in vivo* by 19F NMR. Br J Cancer. 1984;50(1):113-7.

45. <Dietary Restriction of Caenorhabditis elegans by Axenic Culture.pdf>.

46. Sedighi M, Zahedi Bialvaei A, Hamblin MR, Ohadi E, Asadi A, Halajzadeh M, et al. Therapeutic bacteria to combat cancer; current advances, challenges, and opportunities. Cancer Med. 2019;8(6):3167-81.